International Journal of Developmental Neuroscience 79 (2019) 11–20

Contents lists available at ScienceDirect

International Journal of Developmental Neuroscience

journal homepage: www.elsevier.com/locate/ijdevneu

Quantitative MRI study of infant regional brain size following surgery for long-gap esophageal atresia requiring prolonged critical care☆

Chandler Rebecca Lee Mongerson[a], Russell William Jennings[b,c], David Zurakowski[a,b,c], Dusica Bajic[a,b,c,*]

[a] Department of Anesthesiology, Critical Care and Pain Medicine, Boston Children's Hospital, Bader 3, 300 Longwood Ave., Boston, MA, United States
[b] Esophageal and Airway Treatment Center, Department of Surgery, Boston Children's Hospital, 300 Longwood Ave., Boston, MA, United States
[c] Harvard Medical School, 25 Shattuck St., Boston, MA, United States

ARTICLE INFO

Keywords:
Long-gap esophageal atresia
Full-term
Postoperative pain
Sedation
Term
Tolerance

ABSTRACT

Introduction: Little is known regarding the impact of concurrent critical illness and thoracic noncardiac perioperative critical care on postnatal brain development. Previously, we reported smaller total brain volumes in both critically ill full-term and premature patients following complex perioperative critical care for long-gap esophageal atresia (LGEA). Our current report assessed trends in regional brain sizes during infancy, and probed for any group differences.

Methods: Full-term (n = 13) and preterm (n = 13) patients without any previously known neurological concerns, and control infants (n = 16), underwent non-sedated 3 T MRI in infancy (< 1 year old). T2-weighted images underwent semi-automated brain segmentation using Morphologically Adaptive Neonatal Tissue Segmentation (MANTiS). Regional tissue volumes of the forebrain, deep gray matter (DGM), cerebellum, and brainstem are presented as absolute (cm3) and normalized (% total brain volume (%TBV)) values. Group differences were assessed using a general linear model univariate analysis with corrected age at scan as a covariate.

Results: Absolute volumes of regions analyzed increased with advancing age, paralleling total brain size, but were significantly smaller in both full-term and premature patients compared to controls. Normalized volumes (%TBV) of forebrain, DGM, and cerebellum were not different between subject groups analyzed. Normalized brainstem volumes showed group differences that warrant future studies to confirm the same finding.

Discussion: Both full-term and premature critically ill infants undergoing life-saving surgery for LGEA are at risk of smaller total and regional brain sizes. Normalized volumes support globally delayed or diminished brain growth in patients. Future research should look into neurodevelopmental outcomes of infants born with LGEA.

1. Introduction

Rapid and dynamic brain growth and maturation throughout the first year of life is sensitive to environmental/external stimuli (Tierney and Nelson, 2009). Studies of early brain plasticity suggest early exposure to stressors (e.g. procedural pain or prolonged exposure to analgesic medications) in the neonatal intensive care unit (NICU) may disrupt the normal interplay of brain maturation processes (Anand and Scalzo, 2000; Doesburg et al., 2013; Duerden et al., 2018; Hauser and Knapp, 2017; Smith et al., 2011). Disruption of time-sensitive neurodevelopmental events can result in delayed brain maturation and have been implicated in poor long-term developmental outcomes (Atkinson and Braddick, 2007; Bjuland et al., 2013; Howard et al., 2011; Martinussen et al., 2005; Pineda et al., 2013; Skranes et al., 2012; Zubiaurre-Elorza et al., 2012) and psychiatric disorders (Ecker et al., 2013; Greenstein et al., 2006). Notably, prematurity – defined as birth < 37 weeks gestational age (GA) – is associated with increased risk of adverse neurologic sequelae, manifesting as cognitive (Atkinson and Braddick, 2007; Howard et al., 2011; Ortibus et al., 2012) and behavioral (Bruggink et al., 2008; Grunau et al., 1994; Pineda et al., 2013) disorders later in life. Moreover, it is frequently assumed that full-term gestation is neuroprotective. However, emerging evidence

Abbreviations: CSF, cerebrospinal fluid; DGM, deep gray matter; ECMO, extracorporeal membrane oxygenation; FAST, FMRIB's Automated Segmentation Tool; FSL, FMRIB Software Library; GA, gestational age; GLM, general linear model; LGEA, long-gap esophageal atresia; MANTiS, Morphologically Adaptive Neonatal Tissue Segmentation; MRI, magnetic resonance imaging; NICU, neonatal intensive care unit; SPSS, Statistical Package for the Social Sciences; TBV, total brain volume

☆ Supported by NIDAK08 DA035972-01 and Trailblazer Award (D. Bajic).

* Corresponding author at: Department of Anesthesiology, Critical Care and Pain Medicine, Boston Children's Hospital, 300 Longwood Avenue, Bader 3, Boston, MA, 02115, United States.
E-mail address: dusica.bajic@childrens.harvard.edu (D. Bajic).

https://doi.org/10.1016/j.ijdevneu.2019.09.005
Received 2 June 2019; Received in revised form 5 September 2019; Accepted 23 September 2019
Available online 26 September 2019

implicates critical illness (e.g. chronic lung disease, patent ductus arteriosus, postnatal infection, and need for mechanical ventilation) as an important risk factor for altered regional brain development irrespective of prematurity (Bonifacio et al., 2010; Shim et al., 2012).

For infants born with congenital diaphragmatic hernia, many studies report extracorporeal membrane oxygenation (ECMO) as a potential risk factor for higher rates of adverse neurodevelopmental outcomes (Ahmad et al., 1999; McGahren et al., 1997). However, there are limited data regarding short- and long-term sequelae in infants born with noncardiac congenital anomalies undergoing thoracic surgery without ECMO. Recent investigations reported higher incidence of brain injury (Stolwijk et al., 2017) and long-term neurodevelopmental delay (Laing et al., 2011; Stolwijk et al., 2016) following neonatal surgery and complex critical care. At Boston Children's Hospital, the Esophageal and Airway Treatment Center afforded the opportunity to study a unique population of full-term and premature infants born with gastrointestinal congenital anomalies (viz. long-gap esophageal atresia (LGEA) (Bairdain et al., 2015; Kunisaki and Foker, 2012)) that require surgical treatment without the confounding variable of ECMO as part of perioperative critical care management. Using noninvasive magnetic resonance imaging (MRI), our previous report (Mongerson et al., 2019) showed (1) qualitative brain findings with constellation of signs implicating brain atrophy and (2) disproportionately smaller total brain volume and larger extra-axial spaces in both full-term and premature patients following complex perioperative treatment for LGEA that included Foker process (Foker et al., 2009; Kunisaki and Foker, 2012) and prolonged sedation (≥5 days) with opioids and benzodiazepines to facilitate postoperative mechanical ventilation. Sedation in infancy ≥5 days is associated with pharmacological dependence to sedative agents (Solodiuk et al., 2019). Our aim in the present study was to further investigate regional brain volumes (viz. total forebrain, forebrain deep gray matter, cerebellum and brainstem) in aforementioned patient population using the novel Morphologically Adaptive Neonatal Tissue Segmentation (MANTiS) tool (Beare et al., 2016). In this cross-sectional study, we assessed trends in regional brain sizes during infancy, and probed for any group differences.

2. Methods

2.1. Study design and participants

We conducted a pilot infant MRI study with ethical approval from Boston Children's Hospital Institutional Review Board (IRB-P000007855) as a 'no more than minimal risk' study. Informed written parental consent was obtained prior to participation, in accordance with the Declaration of Helsinki and Good Clinical Practice guidelines. Family of each subject received a $90 gift card for subject's participation in the non-sedated research brain MRI scan. Eligibility criteria included < 1-year-old full-term (37–42 weeks GA at birth) and moderate-to-late preterm (28–36 weeks GA at birth) patients who underwent thoracic noncardiac surgery for gastrointestinal congenital anomalies (viz. Foker process for LGEA repair (Bairdain et al., 2015; Kunisaki and Foker, 2012)). Complex postoperative critical care included: (1) prolonged sedation (≥5 days) to facilitate postoperative mechanical ventilation, which resulted in pharmacological dependence to sedative agents (Anand et al., 1999; Dewey, 1984; Solodiuk et al., 2019) and (2) subsequent weaning from sedation medications (viz. opioids and benzodiazepines). Although we did not analyze potential symptoms of withdrawal or withdrawal prevention management (for Review on weaning treatment see (Vet et al., 2016)), we confirmed administration of opioids and benzodiazepines was indicated specifically for weaning management as per primary team and/or pain service consult notes. Representative timeline illustrating sequence of perioperative critical care was presented elsewhere (Hodkinson et al., 2019; Mongerson et al., 2019). Healthy full-term infants with no prior exposure to surgery, anesthesia or sedation were also recruited as a reference baseline for typical infant brain development. Controls were recruited from a pool of Boston Children's Hospital outpatients and two newborn centers (Beth Israel Deaconess Medical Center and Brigham and Women's Hospital) via fliers and advertisement. Exclusion criteria included: (1) extreme prematurity (< 28 weeks GA at birth); (2) cardiac surgeries and/or ECMO exposure; (3) cranial ultrasound findings (e.g. ventricular enlargement with or without gray matter and/or ventricular hemorrhage); (4) neurological disease (e.g. seizures); (5) chromosomal abnormalities (e.g. Down syndrome); (6) prenatal drug

Table 1
Recruitment and Group Characteristics.

n	Controls	Full-Term Patients	Premature Patients
Recruitment Process			
Considered/(Chart) Reviewed	61	173	108
Eligible (%Reviewed)	58 (95%)	63 (36%)	49 (45%)
Approached (%Eligible)	55 (95%)	40 (63%)	23 (47%)
Consented (%Approached)	21 (38%)	19 (48%)	18 (78%)
Scanned (%Consented)	21 (100%)	13 (68%)	13 (72%)
Included/Analyzed (%Scanned)	**16 (76%)**	**13 (100%)**	**13 (100%)**
Demographic Characteristics			
Sex (male), n (%)	15 (94%)	7 (54%)	8 (62%)
Average GA at birth (weeks) ± SD	39.2 ± 1.2	38.5 ± 1.1	32.2 ± 2.9
Median CA at scan [range] (months)	3.2 [0.5–11.7]	5.4 [0.7–13.0]	3.8 [1.4–7.5]
Multiple births, n (%)	1 (6%)	1 (8%)	2 (15%)
Primary diagnoses			
Isolated LGEA, n (%)	0	3 (23%)	3 (23%)
LGEA with TEF, n (%)	0	5 (38%)	9 (69%)
Other, n (%)	0	5 (38%)	1 (8%)

Table 1 summarizes study recruitment process for the 3 groups (controls, and full-term and preterm patients), as well as demographic and clinical characteristics of all subjects included in the T2-weighted analysis. Out of all eligible subjects, 28% (16/58) of controls, 21% (13/63) of full-term patients, and 27% (13/49) of premature patients were successfully scanned and data was analyzed. Primary diagnoses are shown stratified based on noncardiac congenital anomaly diagnoses: (1) isolated LGEA, (2) LGEA with TEF, and (3) Other - that included LGEA as part of VACTERL association (without cardiac involvement). Typically, infants diagnosed with VACTERL exhibit ≥3 of the characteristic features (viz. vertebral defects, anal atresia, cardiac defects, tracheo-esophageal fistula, renal anomalies, and limb abnormalities). None of the infants included in analysis had exposure to extracorporeal membrane oxygenation. For other exclusion criteria, see Methods. *Abbreviations*: **GA**, gestational age; **CA**, corrected age; **LGEA**, long-gap esophageal atresia; **TEF**, tracheo-esophageal fistula.

exposure; and/or (7) MRI incompatible implants. Final data analysis included 3 groups: full-term and moderate-to-late preterm patients, and full-term controls. This study is extension of our previous work (Mongerson et al., 2019) with the following changes: (1) addition of two new control subjects (8 and 9 months-old), and (2) replacement follow up scans for 2 previously analyzed infants to improve quality of T2-weighted images used for detailed brain segmentation (3 months-old control subject and 5 months-old full-term patient). Summary of recruitment details (e.g. number of subjects screened, eligible, and enrolled) and group characteristics (demographics and clinical information) are shown in Table 1.

2.2. MRI acquisition

All infants were scanned in late evenings or at night without any sedation using a 3 T TrioTim MRI system equipped with 32-channel receive-only head coil and body-transmission (Siemens Healthcare Inc., USA). Patients' scans were acquired following completion of all treatment, just prior to discharge. Both foam earplugs (Newmatic Medical, Birmingham, AL) and earmuffs (MRI-Safe Neonatal Noise Guards, Universal Medical, Norwood, MA) were placed for noise protection. Infants were also bundled and cradled in MRI-safe Deluxe + carrycot (DockATot, Wilmington, NC), which allowed for easier positioning of sleeping baby into the scanner. Infants were continuously monitored for stable heart rate and oxygenation throughout "feed and wrap" scanning approach. Structural T2-weighted images were collected using an axial fast spin echo sequence (repetition time = 12.62 s; echo time = 110 ms; flip angle = 120°; field of view = 180 × 180 mm^2; 63 slices of 2 mm thickness; voxel size = 0.35 × 0.35 mm^2). T2 images were collected for all scanned full-term and premature patients (n = 13/group), and 16/21 (76%) full-term controls. Of those 16 controls, only one infant had incomplete data collection (partial brain coverage) that precluded analysis of total brain and forebrain volumes (n = 15 healthy controls) but allowed for absolute volume quantification of remaining brain regions - deep gray matter, cerebellum, and brainstem (n = 16 controls). Total number of scans included in the analysis per group is summarized in Table 1.

2.3. Volumetric MRI data analysis

T2-weighted image segmentation was done using **M**orphologically **A**daptive **N**eonatal **Ti**ssue **S**egmentation (MANTiS) toolbox (Beare et al., 2016) as previously described (Mongerson et al., 2019). Since MANTiS (Beare et al., 2016) employs a *neonatal* brain MRI template/atlas (Kuklisova-Murgasova et al., 2011), we used tools in **F**MRIB **S**oftware **L**ibrary (FSL; v.5.0) for additional T2 image preprocessing and post-segmentation editing (see below) in older infants.

2.3.1. Preprocessing

(i) Intracranial space segmentation: T2 images were skull-stripped using "Simple Watershed Scalping" module in the MANTiS toolbox followed by manual editing in FSLview as needed; (ii) Bias field-correction using **F**MRIB's **A**utomated **S**egmentation **T**ool (FAST) (Zhang et al., 2001) was done to improve subsequent registration and tissue segmentation; and (iii) Setting image origin using "Origin to Center of Mass" module in the MANTiS toolbox.

2.3.2. MANTiS Segmentation

Preprocessed intracranial images underwent the MANTiS segmentation pipeline (Beare et al., 2016), which produced probabilistic tissue segmentations. Four out of 8 final automated MANTiS tissue classifications (viz. cortical gray and white matter delineations, hippocampus and amygdala) were not evaluated in this study due to unreliable output segmentations in older infants. In turn, we analyzed the remaining 4 tissue segmentations: cerebrospinal fluid (CSF; data previously reported, see Fig. 4 in (Mongerson et al., 2019)), deep gray matter (DGM), cerebellum, and brainstem (Fig. 1). Analysis of CSF was needed for calculation of total brain mask (Fig. 1A) as difference between intracranial space and CSF volumes (see below).

2.3.3. Post-segmentation editing

Selected regions of interest were visually inspected and noted tissue misclassifications found for older infants were edited as follows:

(1) **CSF segmentation:** Output was (i) masked to zero voxels outside the intracranial space, (ii) thresholded at 40% to eliminate voxels with < 40% probability of representing CSF, and (iii) converted to a binary mask. CSF masks underwent additional (iv) complex editing. Namely, a CSF partial volume estimate generated by FAST (see 2.3.1. **Preprocessing** above) was (a) thresholded at 50% to eliminate voxels with < 50% of their volume comprising CSF, (b) converted to a binary mask, and then (c) combined with MANTiS's thresholded/binarized CSF mask to create a 'comprehensive' CSF image (i.e. all CSF accounted for in previously excluded cisterns, 4th ventricle, and sulcal spaces). Finally, the latter underwent additional minor (d) manual editing to erase remaining misclassified hyperintense brain tissue. Details of CSF results are reported elsewhere (Mongerson et al., 2019).

(2) **Brain regions' segmentations:** Automated probabilistic maps of the DGM, cerebellum and brainstem, were (i) masked to zero voxels outside the intracranial space to exclude rare inclusion of background voxels in tissue segmentations, (ii) thresholded at 50% (eliminating voxels with < 50% probability of representing respective tissues), and (iii) converted to binary masks for subsequent (iv) manual editing. Specifically, segmentation masks were visualized overlaid on anatomical T2 images using ITK-SNAP (Yushkevich et al., 2006) (www.itksnap.org) and manual editing was applied as per following anatomical definitions:
   - ***DGM*:** This MANTiS segmentation includes basal ganglia, thalamus, and intervening internal capsule (Beare et al., 2016). Only minor corrections were applied to DGM segmentations to (i) erase the corpus callosum - if included, (ii) add-in missing edge of the mask (in one case of 9 month-old infant), and (iii) fill internal holes in the mask either manually or using *fslmaths* with -fillh operation. Representative mask of DGM is shown in Fig. 1**C**.
   - ***Cerebellum*:** The cerebellum segmentation (Fig. 1**D**) excluded cerebellar peduncles (Isgum et al., 2015; Zwicker et al., 2016), with cerebellar-brainstem boundary defined as the point at which cerebellar peduncles were thinnest (Luft et al., 1998). Corrections were mostly related to missing cerebellar tissue at the edges in infants older than 3 months of age.
   - ***Brainstem*:** The brainstem segmentation included cerebellar peduncles, with anatomical boundaries enforced as follows: *inferiorly*, beginning inclusion of tissue at the level of the Foramen Magnum; *superiorly*, terminating tracing at the level of mammillary bodies and posterior commissure; *anteriorly*, by CSF cisterns and 3^{red} ventricle; and *posteriorly*, by CSF cisterns and 4^{th} ventricle. Brainstem manual editing was required to erase misclassified surrounding tissues. Representative mask of brainstem is shown in Fig. 1E.

2.3.4. Volumetric analysis

Segmentation volumes of the intracranial space, CSF, DGM, cerebellum, and brainstem were obtained in terminal using *fslstats* with -V operation. Total brain volume (TBV) was calculated as the difference between intracranial space and CSF and served for purpose of normalization. Forebrain volume was calculated as follows: TBV - (cerebellum + brainstem). Volumetric measures for respective brain tissue segmentations are presented in terms of *absolute* (cm^3) and *normalized* volumes (%TBV) (Choe et al., 2013). Normalization using TBV is appropriate for understanding how a brain region of interest changes

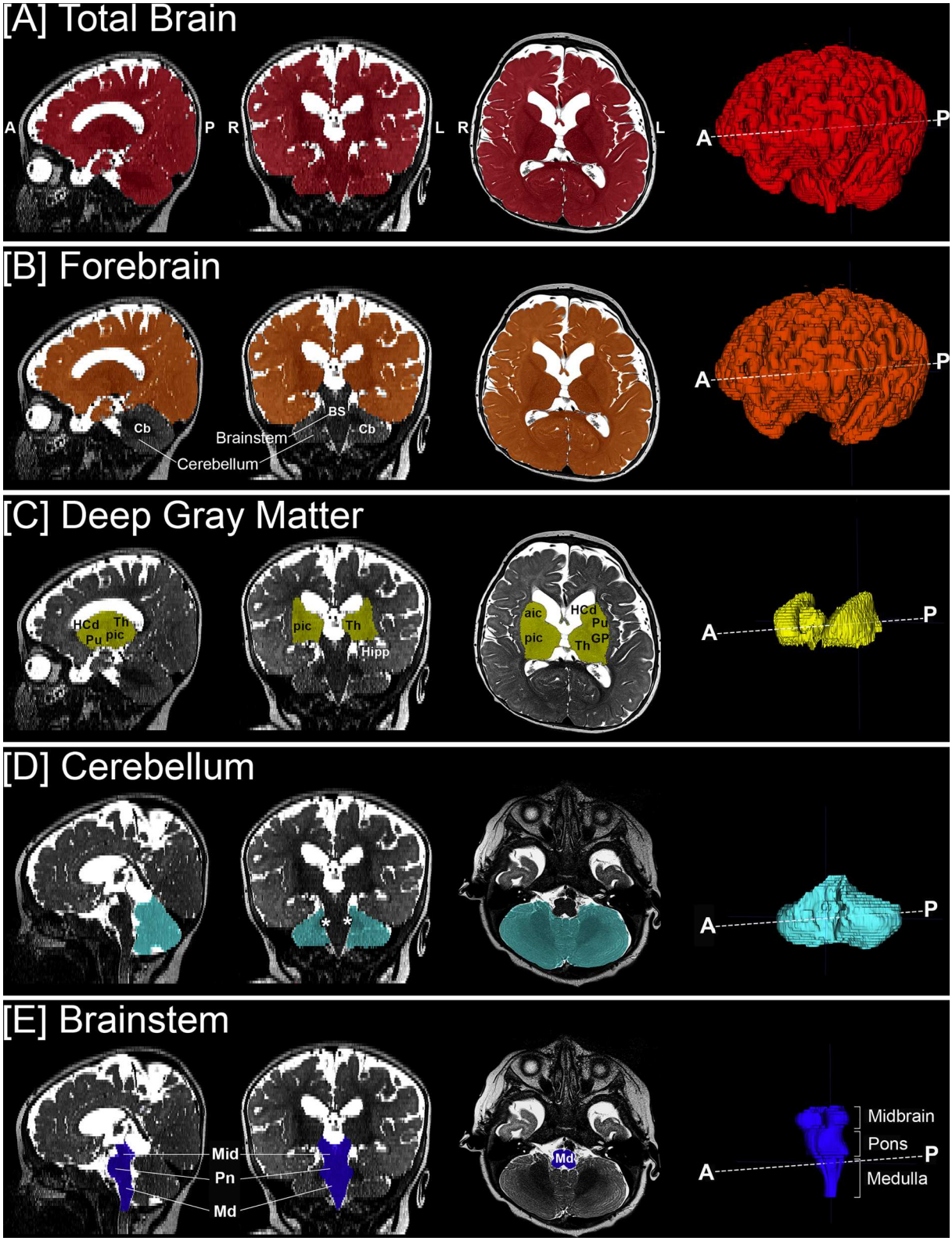

Fig. 1. Brain Segmentation. Representative edited MANTiS segmentations of **(A)** total brain that excludes ventricles (red), **(B)** forebrain (orange), **(C)** deep gray matter (yellow), **(D)** cerebellum (cyan), and **(E)** brainstem (blue) in a full-term patient scanned at 8.9 months of age. Segmentations are shown overlaid on T2-weighted image (gray-scale) in sagittal, coronal, and axial views with corresponding structural 3-D renderings (left to right). Anatomical abbreviations were adopted from previous literature (Paxinos and Watson, 1998). ***Abbreviations***: *, middle cerebellar peduncle; **A**, anterior; **aic**, anterior internal capsule; **BS**, brainstem; **Cb**, cerebellum; **GP**, globus pallidus; **HC**, head of caudate; **Hipp**, hippocampus; **L**, left; **Md**, medulla; **Mid,** midbrain; **P**, posterior; **pic**, posterior internal capsule; **Pn**, pons; **Pu**, putamen; **R**, right; **Th**, thalamus.

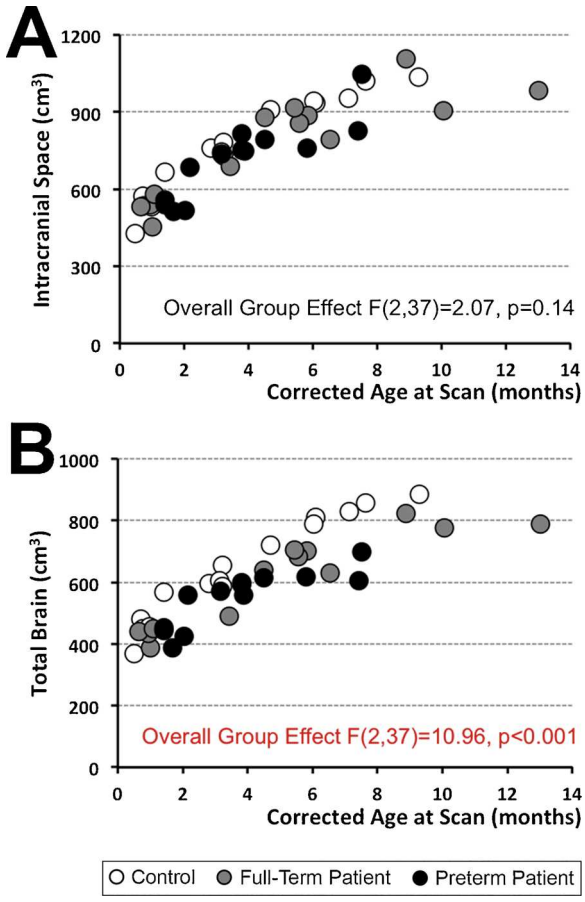

Fig. 2. Intracranial and Total Brain Volumes. Graphs display individual absolute intracranial (as a proxy of head circumference) and total brain volumes (cm^3; excludes ventricles) obtained from T2-weighted MRI scans for the three groups: (1) controls (n = 15; open circles), (2) full-term patients (n = 13; gray circles), and (3) premature patients (n = 13; black circles). Total brain volumes were not available for 1/16 controls (infant scanned at 11.7 months-old) due to partial forebrain coverage. Presented data is updated from our previous work (Mongerson et al., 2019) with addition of two new control subjects (8 and 9 months old), and replacement follow up scans for 2 previously analyzed infants to improve quality of T2-weighted images (3 months-old control subject and 5 months full-term patient). GLM univariate analysis for main effect of group confirmed our previous findings of lack of difference in intracranial volumes between groups ($F(2,37) = 2.07$, $p = 0.14$; **Panel A**), and significantly lower total brain volumes ($F(2,37) = 10.96$, $p < 0.001$) in both full-term and premature patients in comparison to controls ($p < 0.001$), with no differences between patient groups (**Panel B**).

proportionally with respect to the brain as a whole (O'Brien et al., 2011).

2.4. Statistical analysis

As this was a pilot study and no prior information were available regarding the brain volumes in the selected groups of patients with LGEA, a convenience sample size of 13 patients/group was chosen, based on the anticipated number of eligible infants at our institution and an estimated 50% enrollment rate. Statistical analyses were performed using the Statistical Package for the Social Sciences (SPSS; v.23.0, IBM Corporation, Armonk, NY). Normal distribution of continuous variables was confirmed by Shapiro-Wilk test. Both absolute (cm^3) and normalized (%TBV) volumes were related to group status using a general linear model (GLM) univariate analysis with corrected age at scan as a covariate. GLM is a flexible generalization of ordinary linear regression that allows for response variables that have error distribution models other than a normal distribution (McCullagh and Nelder, 1989). Specifically, we evaluated the main effect of group and of age at scan, as well as group by age interactions for all variables. Statistical significance was assessed at the $\alpha < 0.05$.

3. Results

Brain segmentation of T2-weighted images (Fig. 1) allowed for volumetric comparisons between full-term and premature patients, and full-term controls (Table 1). Absolute intracranial ($F(1,37) = 139.40$, $p < 0.001$) and total brain volumes ($F(1,37) = 180.47$, $p < 0.001$) increased with advancing age for all groups (Fig. 2**A** and **B**, respectively). Only total brain volume, but not intracranial volume - a proxy of head circumference, was significantly smaller in both patient groups when compared to controls (statistical details in Fig. 2). Such findings are consistent with our previous report (Mongerson et al., 2019) after addition of 2 new controls and replacement follow up scans for 2 previously analyzed infants to improve quality of T2-weighted images. Obtained total brain volumes (Fig. 2B) were used for subsequent normalization of regional brain structural volumes.

3.1. Absolute regional brain volumes

Representative brain segmentations used for regional brain volume analysis of forebrain, DGM, cerebellum, and brainstem are illustrated in Fig. 1**B–E**. Similar to total brain size, absolute volumes (cm^3) of all regional structures significantly increased with advancing age irrespective of group status (Fig. 3, left panels): forebrain ($F(1,37) = 160.00$, $p < 0.001$), DGM ($F(1,38) = 83.23$, $p < 0.001$), cerebellum ($F(1,38) = 319.26$, $p < 0.001$), and brainstem ($F(1,38) = 117.87$, $p < 0.001$), confirming regional brain growth with age in both patients' groups and controls. Significant interaction between age at scan and group status was observed for absolute volumes of forebrain ($F(2,35) = 5.42$, $p = 0.009$), DGM ($F(2,36) = 5.91$, $p = 0.006$), and cerebellum ($F(2,36) = 7.10$, $p = 0.003$), but not the brainstem ($F(2,36) = 1.06$, $p = 0.36$). These findings suggest altered group trends in regional brain sizes over time for all brain regions analyzed except the brainstem. Lastly, absolute volumes of all brain regions were significantly lower in both full-term and premature patients in comparison to controls ($p \leq 0.002$) with no differences between patient groups (statistical details in Fig. 3, left panels).

3.2. Normalized regional brain volumes

Analysis of normalized regional brain volumes as %TBV accounts for individual differences in global brain size, allowing for detection of disproportionate volumetric changes of certain structures over time (Fig. 3, right panels). Normalized volumes of regional structures significantly decreased with advancing age in infancy for forebrain ($F(1,37) = 93.99$, $p < 0.001$), DGM ($F(1,37) = 18.97$, $p < 0.001$), and brainstem ($F(1,37) = 7.77$, $p = 0.008$) while those of the cerebellum increased ($F(1,37) = 117.51$, $p < 0.001$). No significant interactions between age at scan and group status were observed for any of the structures: forebrain ($F(2,35) = 0.73$, $p = 0.49$), DGM ($F(2,35) = 2.71$, $p = 0.08$), cerebellum ($F(2,35) = 0.67$, $p = 0.52$), or brainstem ($F(2,35) = 1.40$ $p = 0.26$), which suggests similar trend lines in regional brain sizes between groups over time. Similarly, no group differences were observed in normalized volumes for forebrain, DGM and cerebellum (statistical details in Fig. 3**A–C**, right panels). In contrast, normalized brainstem volumetric analysis (Fig. 3D, right panel) showed differences between full-term patients and controls ($p = 0.008$) and full-term and preterm patients ($p = 0.04$), but not between preterm patients and controls ($p = 0.59$). Even though brainstem analysis indicated potential group differences, clinically, value differences in normalized brainstem volumes are very small and should be interpreted with caution.

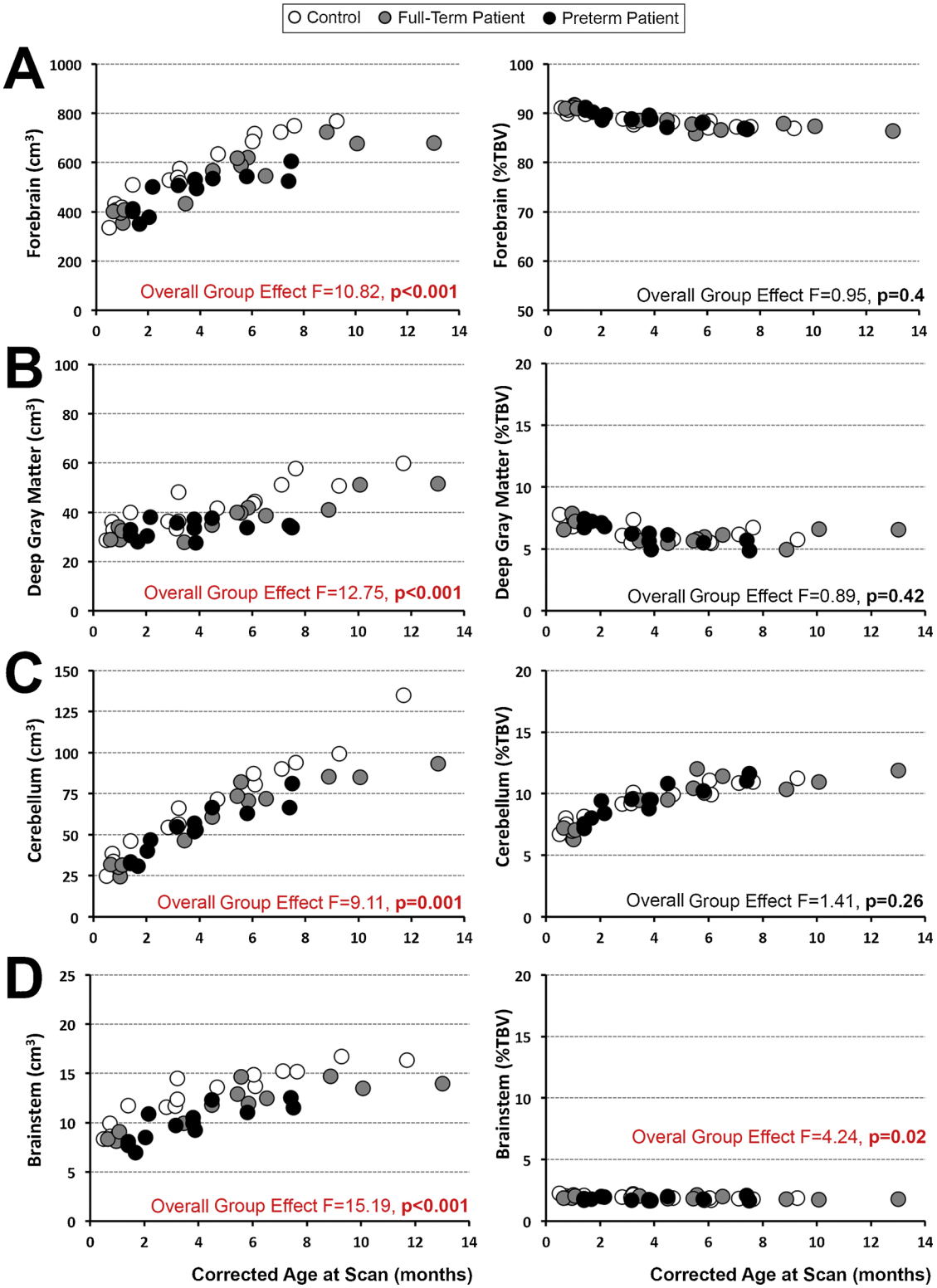

Fig. 3. Regional Brain Volumes. Graphs display individual absolute (cm^3, left panels) and normalized volumes as a % total brain volume (%TBV, right panels) for the three groups: (1) controls (n = 16; open circles), (2) full-term patients (n = 13; gray circles), and (3) premature patients (n = 13; black circles). Total brain (for normalization) and forebrain volumes were not available for 1/16 controls (infant scanned at 11.7 months-old) due to incomplete brain coverage. GLM univariate analysis of **absolute volumes** for main effect of group (left panels) showed significant differences: **(A)** forebrain ($F(2,37) = 10.82$, $p < 0.001$), **(B)** deep gray matter (DGM; $F(2,38) = 12.75$, $p < 0.001$), **(C)** cerebellum ($F(2,38) = 9.11$, $p = 0.001$), and **(D)** brainstem ($F(2,38) = 15.19$, $p < 0.001$). Specifically, absolute volumes of all structures were significantly lower in patients in comparison to controls ($p \leq 0.002$) with no significant differences detected between full-term and premature patients. **Normalized volumes** (right panels) of forebrain, DGM and brainstem significantly decreased with advancing age, while those of the cerebellum increased. No main effect of group was detected for normative volumes of forebrain, DGM, and cerebellum. Analysis showed significant group differences in normalized brainstem volumes ($F(2,37) = 4.24$, $p = 0.02$) between full-term patients and controls ($p = 0.008$) and full-term and preterm patients ($p = 0.04$), but not preterm patients and controls ($p = 0.59$). Since clinical value differences in normalized brainstem volumes are very small, they should be interpreted with caution.

4. Discussion

This report extends our previous qualitative and quantitative findings of lower TBV and greater CSF in full-term and premature patients following perioperative care for LGEA in the absence of difference in intracranial volume, a proxy of head circumference (Mongerson et al., 2019). Specifically, we show smaller absolute regional brain volumes in patients compared to control infants with no heightened vulnerability of forebrain, deep gray matter or cerebellum suggesting generalized reduction in global brain size.

4.1. Infant total and regional brain volumes

Although previous volumetric studies at early ages (Choe et al., 2013; Gilmore et al., 2007; Knickmeyer et al., 2008; Matsuzawa et al., 2001) have provided invaluable information about early brain development, to our knowledge, our current report is the first quantitative study that provides information on regional brain size in the setting of thoracic noncardiac perioperative critical care. We report smaller regional brain volumes that paralleled smaller TBV implicating global brain atrophy in both full-term and premature infants following LGEA treatment. Such findings suggest that brain development – not only in premature, but in *full-term* infants might be affected by the critical illness and complex perioperative treatment for LGEA that involves Foker Process (Foker et al., 2009; Kunisaki and Foker, 2012), repeated anesthesia and prolonged sedation.

4.1.1. Absolute brain volumes

We show that absolute volumes of all explored brain regions (forebrain, DGM, cerebellum, and brainstem) increased with advancing age, but were significantly smaller in both full-term and premature patients following thoracic noncardiac perioperative critical care for LGEA when compared to controls, with no differences between patient groups (Fig. 3, left panels). The overall high rate of postnatal brain growth in the first year of life has been extensively reported for TBV (Gilmore et al., 2012; Knickmeyer et al., 2008; Shi et al., 2011) and its 'sub-regions' (Choe et al., 2013; Gilmore et al., 2018; Peterson et al., 2003). Indeed, study by Choe et al. (2013), which involved detailed manual segmentation of global and discrete anatomical structures, reported that absolute volume increases from 3 to 13 months of age for all brain regions (except for midbrain). Effect of prematurity on regional brain growth has been well documented. A retrospective study in moderately premature infants (born at 30–35 weeks GA) (Niwa et al., 2017) reported smaller cerebral hemispheres and DGM, but not cerebellar and brainstem volumes, in comparison to full-term infants scanned at term-equivalent age. Furthermore, prematurity has been repeatedly implicated in smaller DGM volumes at term-equivalent age (Boardman et al., 2006; Inder et al., 2005; Loh et al., 2017; Srinivasan et al., 2007) associated with poorer neurodevelopmental outcomes at 7 years of age (Loh et al., 2017). Another study in premature infants found a strong correlation between cumulative opioid dose and incidence of cerebellum injury and size, even after adjusting for major confounds including prematurity at birth and elements of clinical care (McPherson et al., 2015). Similar study in very preterm infants by Zwicker et al. (2016) reported a strong correlation between cumulative opioid treatment and cerebellar volume, impaired cerebellar growth in the neonatal period, and poorer motor and cognitive neurodevelopmental outcomes in early childhood. Interestingly, authors did not find such correlation for total brain volume or several sub-tissues therein (cortical gray and white matter, and DGM). However, none of these studies looked into regional brain volumes of infants undergoing complex perioperative critical care with prolonged sedation as presented in this report.

4.1.2. Normalized brain volumes

Relative to total brain tissue, normative volumes of forebrain, DGM, and cerebellum did not differ between the groups. Although brainstem analysis indicated potential significant group differences (full-term patients were different from both controls and premature patients), normalized brainstem values show numerically very small differences and should be interpreted with caution. Future studies with more power and narrower clinical criteria for inclusion in premature patients should be considered. Importantly, trajectories of all normalized volumes followed those previously reported in the literature for normally developing full-term infants across the first year of life (Choe et al., 2013). Although brain regions analyzed were more refined in study by Choe et al. (2013), authors reported normalized values decreased without gender differences for cerebrum, thalamus, and brainstem, and proportionally increased without a gender effect for cerebellum. Our results are consistent with these findings.

4.2. Brain findings in thoracic noncardiac congenital anomalies

To date, infants with noncardiac congenital anomalies have not been extensively investigated. Recent report by Stolwijk et al. (2017) revealed mild to moderate brain abnormalities in 58% of full-term and 75% of premature infants. Only 37% of infants with gastrointestinal abnormalities were without any brain lesions. In addition to prematurity, authors concluded that the type of congenital anomaly seemed to be the best predictor of parenchymal lesions, with up to 53% of infants with esophageal atresia displaying qualitative lesions on MRI (parenchymal lesions in 36% and nonparenchymal abnormalities in 24%). Our previous work in the cohort of patients in current study reported qualitative MRI findings with 46%-*possible* and 54%-*very likely* brain atrophy in full-term patients with LGEA (see Fig. 6 in (Mongerson et al., 2019)). Many studies have shown that prematurity is associated with smaller total brain volumes (Gui et al., 2018), which in turn is associated with poorer long-term outcomes (Cheong et al., 2013, 2016; Keunen et al., 2016). Furthermore, early MRI brain tissue volumes are reportedly strongly predictive of long-term neurodevelopmental outcomes (Cheong et al., 2016; Narberhaus et al., 2007; Rose et al., 2015). Indeed, literature is supportive of using early neuroimaging in predicting neurodevelopmental outcomes (El-Dib et al., 2010; Kwon et al., 2014; Peterson et al., 2003; Woodward et al., 2006). Future studies in this vulnerable clinical population of full-term and premature infants with LGEA should also include diffusion tensor imaging and tractography to shed light on possible mechanisms underlying implied decreased global brain growth. Future longitudinal neurodevelopmental follow up will help us understand the neurocognitive correlates of presented structural findings.

4.3. Study limitations

Several limitations should be addressed when interpreting presented results.

4.3.1. Study groups

This study lacked a true control group due to the absence of infants with similar non-cardiac LGEA that undergo alternate treatment. We were not able to recruit infants that received only prolonged sedation (without surgery), nor premature infants that did not require medical care. Although infants with known brain abnormalities and neurologic disease were excluded from this study, there are no pretreatment MRIs available to rule out inherently smaller brains in subjects analyzed. Notably, studies in infants with congenital diaphragmatic hernia requiring cardiac surgery with ECMO exposure have shown brain abnormalities *prior* to cardiac surgery (Ortinau et al., 2013). Second, patients with LGEA without cardiac involvement are somewhat heterogeneous group because of individual level of underlying disease and treatment complexity. Because cases of LGEA cohort are rare, we pooled them together since they all share requirement for Foker process necessitating prolonged sedation associated with development of

dependence to sedation drugs (viz. opioids and benzodiazepines). While sex distributions in patient groups were balanced, the control group was predominantly comprised of males. Given reported sex-dependent relationships of whole brain sizes (Benavides et al., 2019; Holland et al., 2014; Thompson et al., 2018), future studies with increased power should look into gender differences. Of note, one study found that normalization of regional brain volumes (%TBV) reportedly corrected for sex-specific differences, with the exception of caudate and cerebellar vermis for which a Male < Female relationship persisted (Choe et al., 2013). Finally, this is a single center study from Esophageal and Airway Treatment Center at Boston Children's Hospital, and future multicenter studies are needed to confirm presented results. Predefined perinatal and several potentially relevant perioperative risk factors in the pathogenesis of or susceptibility to global decreased brain size should be investigated in future studies (e.g. hypoglycemia, cerebral perfusion, hypocarbia, length of mechanical ventilation and sedation, cumulative anesthesia exposure, vasopressor treatment, culture-proven sepsis).

4.3.2. MRI acquisition challenge in non-sedated infants

Although motion during MRI acquisition remains a significant challenge (Gao et al., 2014; Hughes et al., 2017), our efforts to refine scan protocols allowed for improved rates of successful scan completion (100% scanned patients). We noted only very minor head motion, such as single slice disruption (e.g. easily approximate artifact-corrupted slice using 3D rendering tool in ITK-SNAP) or slight ringing artifact. In total, described minor motion artifacts were seen in a limited number of infants: 2/16 controls, 2/13 full-term patients and 3/13 preterm patients. Given incidences were roughly evenly dispersed across groups and the low probability that such minor artifacts would impact gross brain volume estimations, the decision was made to include these subjects.

4.3.3. Methodological considerations of infant brain segmentation

In this study, we employed the previously developed neonatal brain segmentation tool MANTiS (Beare et al., 2016). Since MANTiS employs a *neonatal* brain MRI template/atlas (Kuklisova-Murgasova et al., 2011), extensive editing of automated segmentations was needed prior to volumetric quantification in older infants (> 4 months of age). For example, evolving tissue contrasts in the first year of life due to ongoing myelination may have contributed to inclusion of corpus callosum in DGM segmentations of older infants. Furthermore, due to poor signal-to-noise ratio between developing gray matter and unmyelinated tracts on MRI – compounded with the continuum of ongoing myelination across the first year of life – we were not able to accurately analyze separate cortical gray and white matter volumes. Similarly, compounded with poor reliability of automated segmentations for smaller nuclei of hippocampus and amygdala, we chose to include those tissue classifications as part of the forebrain volume (comprised of cortical gray and white matter, hippocampus, amygdala, and DGM). Reliability of gray-white matter distinctions in structural MRI images for accurate quantification, particularly in the transitional period between 4 and 8 months of age, currently represents a major technical challenge that remains to be resolved. Since finer anatomical divisions may improve our understanding of brain changes in this unique cohort of infants and their later outcomes, future technical improvements in acquisition parameters and preprocessing tools will be important to better characterize more specific regional brain sizes.

5. Conclusions

This study provides evidence that both *full-term* and *premature* infants with thoracic noncardiac congenital anomalies (viz. LGEA) undergoing surgery and complex critical care involving prolonged sedation are at risk of globally decreased or delayed brain growth. In addition to careful perioperative and critical care monitoring of vital signs and neurologic function as part of the standard of care, clinical teams should consider neuroimaging of infants with LGEA before and/or following Foker process since head circumference might not represent the best measure for this unique cohort of infants. Additional research is warranted into potential mechanisms of presented smaller regional brain sizes and potential long-term neurodevelopmental outcomes.

Author Contributions

Authorship credit was based on substantial contributions to (1) the conception and manuscript design (CRLM and DB); (2) acquisition (CRLM, RWJ, and DB), analysis (CRLM, DZ, and DB), or interpretation of data (all authors); (3) drafting the article (CRLM and DB) or critical revision for important intellectual content (all authors); (4) final approval of the version to be published (all authors); and (5) are accountable for all aspects of the work in ensuring that questions related to the accuracy or integrity of any part of the work are appropriately investigated and resolved (all authors).

Declaration of Competing Interest

None.

Acknowledgments

This work was supported by the NIDAK08 DA035972-01 (NIH, United States) and *Trailblazer Award* from the Department of Anesthesiology, Critical Care and Pain Medicine, Boston Children's Hospital, Boston, MA, United States (DB). The authors express tremendous gratitude to infants and their parents for participation in our study. Authors would also like to thank: (i) Dorothy Gallagher, RN and Jean Solodiuk, RN, PhD for their help with recruitment; (ii) Kristina Pelkola BS, RT and Dianne Biagotti, BS, RT for MRI facilitating scheduling in the evenings and week-ends; (iii) All MRI technologists for their invaluable help with scanning; and last but not least (iv) Colleagues from the Fetal-Neonatal Neuroimaging & Developmental Science Center (FNNDSC) for their technical support. The content of this article is solely the responsibility of the authors and does not necessarily represent the official views of the National Institutes of Health.

References

Ahmad, A., Gangitano, E., Odell, R.M., Doran, R., Durand, M., 1999. Survival, intracranial lesions, and neurodevelopmental outcome in infants with congenital diaphragmatic hernia treated with extracorporeal membrane oxygenation. J. Perinatol. 19, 436–440.

Anand, K.J., Barton, B.A., McIntosh, N., Lagercrantz, H., Pelausa, E., Young, T.E., Vasa, R., 1999. Analgesia and sedation in preterm neonates who require ventilatory support: results from the NOPAIN trial. Neonatal outcome and prolonged analgesia in neonates. Arch. Pediatr. Adolesc. Med. 153, 331–338.

Anand, K.J., Scalzo, F.M., 2000. Can adverse neonatal experiences alter brain development and subsequent behavior? Biol. Neonate 77, 69–82.

Atkinson, J., Braddick, O., 2007. Visual and visuocognitive development in children born very prematurely. Prog. Brain Res. 164, 123–149.

Bairdain, S., Hamilton, T.E., Smithers, C.J., Manfredi, M., Ngo, P., Gallagher, D., Zurakowski, D., Foker, J.E., Jennings, R.W., 2015. Foker process for the correction of long gap esophageal atresia: primary treatment versus secondary treatment after prior esophageal surgery. J. Pediatr. Surg. 50, 933–937.

Beare, R.J., Chen, J., Kelly, C.E., Alexopoulos, D., Smyser, C.D., Rogers, C.E., Loh, W.Y., Matthews, L.G., Cheong, J.L., Spittle, A.J., Anderson, P.J., Doyle, L.W., Inder, T.E., Seal, M.L., Thompson, D.K., 2016. Neonatal brain tissue classification with morphological adaptation and unified segmentation. Front. Neuroinform. 10, 12.

Benavides, A., Metzger, A., Tereschenko, A., Conrad, A., Bell, E.F., Spencer, J., Ross-Sheehy, S., Georgieff, M., Magnotta, V., Nopoulos, P., 2019. Sex-specific alterations in preterm brain. Pediatr. Res. 85, 55–62.

Bjuland, K.J., Lohaugen, G.C., Martinussen, M., Skranes, J., 2013. Cortical thickness and cognition in very-low-birth-weight late teenagers. Early Hum. Dev. 89, 371–380.

Boardman, J.P., Counsell, S.J., Rueckert, D., Kapellou, O., Bhatia, K.K., Aljabar, P., Hajnal, J., Allsop, J.M., Rutherford, M.A., Edwards, A.D., 2006. Abnormal deep grey matter development following preterm birth detected using deformation-based morphometry. Neuroimage 32, 70–78.

Bonifacio, S.L., Glass, H.C., Chau, V., Berman, J.I., Xu, D., Brant, R., Barkovich, A.J., Poskitt, K.J., Miller, S.P., Ferriero, D.M., 2010. Extreme premature birth is not

associated with impaired development of brain microstructure. J. Pediatr. 157, 726–732 e721.
Bruggink, J.L., Einspieler, C., Butcher, P.R., Van Braeckel, K.N., Prechtl, H.F., Bos, A.F., 2008. The quality of the early motor repertoire in preterm infants predicts minor neurologic dysfunction at school age. J. Pediatr. 153, 32–39.
Cheong, J.L., Anderson, P.J., Roberts, G., Burnett, A.C., Lee, K.J., Thompson, D.K., Molloy, C., Wilson-Ching, M., Connelly, A., Seal, M.L., Wood, S.J., Doyle, L.W., 2013. Contribution of brain size to IQ and educational underperformance in extremely preterm adolescents. PLoS One 8, e77475.
Cheong, J.L., Thompson, D.K., Spittle, A.J., Potter, C.R., Walsh, J.M., Burnett, A.C., Lee, K.J., Chen, J., Beare, R., Matthews, L.G., Hunt, R.W., Anderson, P.J., Doyle, L.W., 2016. Brain volumes at term-equivalent age are associated with 2-Year neurodevelopment in moderate and late preterm children. J. Pediatr. 174, 91–97 e91.
Choe, M.S., Ortiz-Mantilla, S., Makris, N., Gregas, M., Bacic, J., Haehn, D., Kennedy, D., Pienaar, R., Caviness Jr., V.S., Benasich, A.A., Grant, P.E., 2013. Regional infant brain development: an MRI-based morphometric analysis in 3 to 13 month olds. Cereb. Cortex 23, 2100–2117.
Dewey, W.L., 1984. Various factors which affect the rate of development of tolerance and physical dependence to abused drugs. NIDA Res. Monogr. 54, 39–49.
Doesburg, S.M., Chau, C.M., Cheung, T.P., Moiseev, A., Ribary, U., Herdman, A.T., Miller, S.P., Cepeda, I.L., Synnes, A., Grunau, R.E., 2013. Neonatal pain-related stress, functional cortical activity and visual-perceptual abilities in school-age children born at extremely low gestational age. Pain 154, 1946–1952.
Duerden, E.G., Grunau, R.E., Guo, T., Foong, J., Pearson, A., Au-Young, S., Lavoie, R., Chakravarty, M.M., Chau, V., Synnes, A., Miller, S.P., 2018. Early procedural pain is associated with regionally-specific alterations in thalamic development in preterm neonates. J. Neurosci. 38, 878–886.
Ecker, C., Ginestet, C., Feng, Y., Johnston, P., Lombardo, M.V., Lai, M.C., Suckling, J., Palaniyappan, L., Daly, E., Murphy, C.M., Williams, S.C., Bullmore, E.T., Baron-Cohen, S., Brammer, M., Murphy, D.G., Consortium, M.A., 2013. Brain surface anatomy in adults with autism: the relationship between surface area, cortical thickness, and autistic symptoms. JAMA Psychiatry 70, 59–70.
El-Dib, M., Massaro, A.N., Bulas, D., Aly, H., 2010. Neuroimaging and neurodevelopmental outcome of premature infants. Am. J. Perinatol. 27, 803–818.
Foker, J.E., Kendall Krosch, T.C., Catton, K., Munro, F., Khan, K.M., 2009. Long-gap esophageal atresia treated by growth induction: the biological potential and early follow-up results. Semin. Pediatr. Surg. 18, 23–29.
Gao, W., Elton, A., Zhu, H., Alcauter, S., Smith, J.K., Gilmore, J.H., Lin, W., 2014. Intersubject variability of and genetic effects on the brain's functional connectivity during infancy. J. Neurosci. 34, 11288–11296.
Gilmore, J.H., Knickmeyer, R.C., Gao, W., 2018. Imaging structural and functional brain development in early childhood. Nat. Rev. Neurosci. 19, 123–137.
Gilmore, J.H., Lin, W., Prastawa, M.W., Looney, C.B., Vetsa, Y.S., Knickmeyer, R.C., Evans, D.D., Smith, J.K., Hamer, R.M., Lieberman, J.A., Gerig, G., 2007. Regional gray matter growth, sexual dimorphism, and cerebral asymmetry in the neonatal brain. J. Neurosci. 27, 1255–1260.
Gilmore, J.H., Shi, F., Woolson, S.L., Knickmeyer, R.C., Short, S.J., Lin, W., Zhu, H., Hamer, R.M., Styner, M., Shen, D., 2012. Longitudinal development of cortical and subcortical gray matter from birth to 2 years. Cereb. Cortex 22, 2478–2485.
Greenstein, D., Lerch, J., Shaw, P., Clasen, L., Giedd, J., Gochman, P., Rapoport, J., Gogtay, N., 2006. Childhood onset schizophrenia: cortical brain abnormalities as young adults. J. Child Psychol. Psychiatry 47, 1003–1012.
Grunau, R.V., Whitfield, M.F., Petrie, J.H., Fryer, E.L., 1994. Early pain experience, child and family factors, as precursors of somatization: a prospective study of extremely premature and fullterm children. Pain 56, 353–359.
Gui, L., Loukas, S., Lazeyras, F., Huppi, P.S., Meskaldji, D.E., Borradori Tolsa, C., 2018. Longitudinal study of neonatal brain tissue volumes in preterm infants and their ability to predict neurodevelopmental outcome. Neuroimage.
Hauser, K.F., Knapp, P.E., 2017. Opiate drugs with abuse liability hijack the endogenous opioid system to disrupt neuronal and glial maturation in the central nervous system. Front. Pediatr. 5, 294.
Hodkinson, D.J., Mongerson, C.R.L., Jennings, R.W., Bajic, D., 2019. Neonatal functional brain maturation in the context of perioperative critical care and pain management. Heliyon 5, e02350.
Holland, D., Chang, L., Ernst, T.M., Curran, M., Buchthal, S.D., Alicata, D., Skranes, J., Johansen, H., Hernandez, A., Yamakawa, R., Kuperman, J.M., Dale, A.M., 2014. Structural growth trajectories and rates of change in the first 3 months of infant brain development. JAMA Neurol. 71, 1266–1274.
Howard, K., Roberts, G., Lim, J., Lee, K.J., Barre, N., Treyvaud, K., Cheong, J., Hunt, R.W., Inder, T.E., Doyle, L.W., Anderson, P.J., 2011. Biological and environmental factors as predictors of language skills in very preterm children at 5 years of age. J. Dev. Behav. Pediatr. 32, 239–249.
Hughes, E.J., Winchman, T., Padormo, F., Teixeira, R., Wurie, J., Sharma, M., Fox, M., Hutter, J., Cordero-Grande, L., Price, A.N., Allsop, J., Bueno-Conde, J., Tusor, N., Arichi, T., Edwards, A.D., Rutherford, M.A., Counsell, S.J., Hajnal, J.V., 2017. A dedicated neonatal brain imaging system. Magn. Reson. Med. 78, 794–804.
Inder, T.E., Warfield, S.K., Wang, H., Huppi, P.S., Volpe, J.J., 2005. Abnormal cerebral structure is present at term in premature infants. Pediatrics 115, 286–294.
Isgum, I., Benders, M.J., Avants, B., Cardoso, M.J., Counsell, S.J., Gomez, E.F., Gui, L., Huppi, P.S., Kersbergen, K.J., Makropoulos, A., Melbourne, A., Moeskops, P., Mol, C.P., Kuklisova-Murgasova, M., Rueckert, D., Schnabel, J.A., Srhoj-Egekher, V., Wu, J., Wang, S., de Vries, L.S., Viergever, M.A., 2015. Evaluation of automatic neonatal brain segmentation algorithms: the NeoBrainS12 challenge. Med. Image Anal. 20, 135–151.
Keunen, K., Isgum, I., Van Kooij, B.J., Anbeek, P., Van Haastert, I.C., Koopman-Esseboom, C., Fieret-van Stam, P.C., Nievelstein, R.A., Viergever, M.A., De Vries, L.S., Groenendaal, F., Benders, M.J., 2016. Brain volumes at term-equivalent age in preterm infants: imaging biomarkers for neurodevelopmental outcome through early school age. J. Pediatr. 172, 88–95.
Knickmeyer, R.C., Gouttard, S., Kang, C., Evans, D., Wilber, K., Smith, J.K., Hamer, R.M., Lin, W., Gerig, G., Gilmore, J.H., 2008. A structural MRI study of human brain development from birth to 2 years. J. Neurosci. 28, 12176–12182.
Kuklisova-Murgasova, M., Aljabar, P., Srinivasan, L., Counsell, S.J., Doria, V., Serag, A., Gousias, I.S., Boardman, J.P., Rutherford, M.A., Edwards, A.D., Hajnal, J.V., Rueckert, D., 2011. A dynamic 4D probabilistic atlas of the developing brain. Neuroimage 54, 2750–2763.
Kunisaki, S.M., Foker, J.E., 2012. Surgical advances in the fetus and neonate: esophageal atresia. Clin. Perinatol. 39, 349–361.
Kwon, S.H., Vasung, L., Ment, L.R., Huppi, P.S., 2014. The role of neuroimaging in predicting neurodevelopmental outcomes of preterm neonates. Clin. Perinatol. 41, 257–283.
Laing, S., Walker, K., Ungerer, J., Badawi, N., Spence, K., 2011. Early development of children with major birth defects requiring newborn surgery. J. Paediatr. Child Health 47, 140–147.
Loh, W.Y., Anderson, P.J., Cheong, J.L.Y., Spittle, A.J., Chen, J., Lee, K.J., Molesworth, C., Inder, T.E., Connelly, A., Doyle, L.W., Thompson, D.K., 2017. Neonatal basal ganglia and thalamic volumes: very preterm birth and 7-year neurodevelopmental outcomes. Pediatr. Res. 82, 970–978.
Luft, A.R., Skalej, M., Welte, D., Kolb, R., Burk, K., Schulz, J.B., Klockgether, T., Voigt, K., 1998. A new semiautomated, three-dimensional technique allowing precise quantification of total and regional cerebellar volume using MRI. Magn. Reson. Med. 40, 143–151.
Martinussen, M., Fischl, B., Larsson, H.B., Skranes, J., Kulseng, S., Vangberg, T.R., Vik, T., Brubakk, A.M., Haraldseth, O., Dale, A.M., 2005. Cerebral cortex thickness in 15-year-old adolescents with low birth weight measured by an automated MRI-based method. Brain 128, 2588–2596.
Matsuzawa, J., Matsui, M., Konishi, T., Noguchi, K., Gur, R.C., Bilker, W., Miyawaki, T., 2001. Age-related volumetric changes of brain gray and white matter in healthy infants and children. Cereb. Cortex 11, 335–342.
McCullagh, P., Nelder, J.A., 1989. Generalized Linear Models, 2nd ed. Chapman and Hall/CRC, Boca Raton.
McGahren, E.D., Mallik, K., Rodgers, B.M., 1997. Neurological outcome is diminished in survivors of congenital diaphragmatic hernia requiring extracorporeal membrane oxygenation. J. Pediatr. Surg. 32, 1216–1220.
McPherson, C., Haslam, M., Pineda, R., Rogers, C., Neil, J.J., Inder, T.E., 2015. Brain injury and development in preterm infants exposed to fentanyl. Ann. Pharmacother. 49, 1291–1297.
Mongerson, C.R.L., Wilcox, S.L., Goins, S.M., Pier, D.B., Zurakowski, D., Jennings, R.W., Bajic, D., 2019. Infant brain structural MRI analysis in the context of thoracic non-cardiac surgery and critical care. Front. Pediatr. 7, 315.
Narberhaus, A., Segarra, D., Caldu, X., Gimenez, M., Junque, C., Pueyo, R., Botet, F., 2007. Gestational age at preterm birth in relation to corpus callosum and general cognitive outcome in adolescents. J. Child Neurol. 22, 761–765.
Niwa, T., Suzuki, K., Sugiyama, N., Imai, Y., 2017. Regional volumetric assessment of the brain in moderately preterm infants (30-35 gestational weeks) scanned at term-equivalent age on magnetic resonance imaging. Early Hum. Dev. 111, 36–41.
O'Brien, L.M., Ziegler, D.A., Deutsch, C.K., Frazier, J.A., Herbert, M.R., Locascio, J.J., 2011. Statistical adjustments for brain size in volumetric neuroimaging studies: some practical implications in methods. Psychiatry Res. 193, 113–122.
Ortibus, E., Verhoeven, J., Sunaert, S., Casteels, I., de Cock, P., Lagae, L., 2012. Integrity of the inferior longitudinal fasciculus and impaired object recognition in children: a diffusion tensor imaging study. Dev. Med. Child Neurol. 54, 38–43.
Ortinau, C., Alexopoulos, D., Dierker, D., Van Essen, D., Beca, J., Inder, T., 2013. Cortical folding is altered before surgery in infants with congenital heart disease. J. Pediatr. 163, 1507–1510.
Paxinos, G., Watson, C., 1998. The Rat Brain in Stereotaxic Coordinates, 4th ed. Academic Press, Orlando, FL.
Peterson, B.S., Anderson, A.W., Ehrenkranz, R., Staib, L.H., Tageldin, M., Colson, E., Gore, J.C., Duncan, C.C., Makuch, R., Ment, L.R., 2003. Regional brain volumes and their later neurodevelopmental correlates in term and preterm infants. Pediatrics 111, 939–948.
Pineda, R.G., Tjoeng, T.H., Vavasseur, C., Kidokoro, H., Neil, J.J., Inder, T., 2013. Patterns of altered neurobehavior in preterm infants within the neonatal intensive care unit. J. Pediatr. 162, 470–476 e471.
Rose, J., Cahill-Rowley, K., Vassar, R., Yeom, K.W., Stecher, X., Stevenson, D.K., Hintz, S.R., Barnea-Goraly, N., 2015. Neonatal brain microstructure correlates of neurodevelopment and gait in preterm children 18-22 mo of age: an MRI and DTI study. Pediatr. Res. 78, 700–708.
Shi, F., Yap, P.T., Wu, G., Jia, H., Gilmore, J.H., Lin, W., Shen, D., 2011. Infant brain atlases from neonates to 1-and 2-year-olds. PLoS One 6, e18746.
Shim, S.Y., Jeong, H.J., Son, D.W., Jeong, J.S., Oh, S.H., Park, S.Y., Ryu, T.H., Kim, Y.B., Cho, Z.H., 2012. Altered microstructure of white matter except the corpus callosum is independent of prematurity. Neonatology 102, 309–315.
Skranes, J., Lohaugen, G.C., Evensen, K.A., Indredavik, M.S., Haraldseth, O., Dale, A.M., Brubakk, A.M., Martinussen, M., 2012. Entorhinal cortical thinning affects perceptual and cognitive functions in adolescents born preterm with very low birth weight (VLBW). Early Hum. Dev. 88, 103–109.
Smith, G.C., Gutovich, J., Smyser, C., Pineda, R., Newnham, C., Tjoeng, T.H., Vavasseur, C., Wallendorf, M., Neil, J., Inder, T., 2011. Neonatal intensive care unit stress is associated with brain development in preterm infants. Ann. Neurol. 70, 541–549.
Solodiuk, J.C., Jennings, R.W., Bajic, D., 2019. Evaluation of postnatal sedation in full-term infants. Brain Sci. 9.

Srinivasan, L., Dutta, R., Counsell, S.J., Allsop, J.M., Boardman, J.P., Rutherford, M.A., Edwards, A.D., 2007. Quantification of deep gray matter in preterm infants at term-equivalent age using manual volumetry of 3-tesla magnetic resonance images. Pediatrics 119, 759–765.

Stolwijk, L.J., Keunen, K., de Vries, L.S., Groenendaal, F., van der Zee, D.C., van Herwaarden, M.Y.A., Lemmers, P.M.A., Benders, M., 2017. Neonatal surgery for noncardiac congenital anomalies: neonates at risk of brain injury. J. Pediatr. 182, 335–341 e331.

Stolwijk, L.J., Lemmers, P.M., Harmsen, M., Groenendaal, F., de Vries, L.S., van der Zee, D.C., Benders, M.J., van Herwaarden-Lindeboom, M.Y., 2016. Neurodevelopmental outcomes after neonatal surgery for major noncardiac anomalies. Pediatrics 137, e20151728.

Thompson, D.K., Kelly, C.E., Chen, J., Beare, R., Alexander, B., Seal, M.L., Lee, K., Matthews, L.G., Anderson, P.J., Doyle, L.W., Spittle, A.J., Cheong, J.L.Y., 2018. Early life predictors of brain development at term-equivalent age in infants born across the gestational age spectrum. Neuroimage.

Tierney, A.L., Nelson 3rd, C.A., 2009. Brain development and the role of experience in the early years. Zero Three 30, 9–13.

Vet, N.J., Kleiber, N., Ista, E., de Hoog, M., de Wildt, S.N., 2016. Sedation in critically ill children with respiratory failure. Front. Pediatr. 4, 89.

Woodward, L.J., Anderson, P.J., Austin, N.C., Howard, K., Inder, T.E., 2006. Neonatal MRI to predict neurodevelopmental outcomes in preterm infants. N. Engl. J. Med. 355, 685–694.

Yushkevich, P.A., Piven, J., Hazlett, H.C., Smith, R.G., Ho, S., Gee, J.C., Gerig, G., 2006. User-guided 3D active contour segmentation of anatomical structures: significantly improved efficiency and reliability. Neuroimage 31, 1116–1128.

Zhang, Y., Brady, M., Smith, S., 2001. Segmentation of brain MR images through a hidden Markov random field model and the expectation-maximization algorithm. IEEE Trans. Med. Imaging 20, 45–57.

Zubiaurre-Elorza, L., Soria-Pastor, S., Junque, C., Sala-Llonch, R., Segarra, D., Bargallo, N., Macaya, A., 2012. Cortical thickness and behavior abnormalities in children born preterm. PLoS One 7, e42148.

Zwicker, J.G., Miller, S.P., Grunau, R.E., Chau, V., Brant, R., Studholme, C., Liu, M., Synnes, A., Poskitt, K.J., Stiver, M.L., Tam, E.W., 2016. Smaller cerebellar growth and poorer neurodevelopmental outcomes in very preterm infants exposed to neonatal morphine. J. Pediatr. 172, 81–87 e82.